Available online at www.sciencedirect.com
ScienceDirect
Polymer 48 (2007) 1490–1499
polymer
www.elsevier.com/locate/polymer

Use of acrylic based surfmers for the preparation of exfoliated polystyrene–clay nanocomposites

Austin Samakande, Patrice C. Hartmann, Valeska Cloete, Ronald D. Sanderson*

UNESCO Associated Centre for Macromolecules, Department of Chemistry and Polymer Science, University of Stellenbosch, Private Bag X1, 7602 Matieland, South Africa

Received 14 February 2006; received in revised form 23 June 2006; accepted 23 July 2006
Available online 12 February 2007

Abstract

Two polymerizable cationic surfactants, (11-acryloyloxyundecyl)dimethyl(2-hydroxyethyl)ammonium bromide (hydroxyethyl surfmer) and (11-acryloyloxyundecyl)dimethylethylammonium bromide (ethyl surfmer), were used for the modification of montmorillonite (MMT) clay. The modification of MMT dispersions was carried out by ion exchange of the sodium ions in Na^+-MMT by surfactants in aqueous media. Modified MMT clays were then dispersed in styrene and subsequently polymerized in bulk by a free-radical polymerization reaction to yield polystyrene–clay nanocomposites. An exfoliated structure was obtained using the ethyl surfmer-modified clay, whereas a mixed exfoliated/intercalated structure was obtained using the hydroxyethyl surfmer-modified clay. Nanocomposite structures were confirmed by small angle X-ray scattering (SAXS) and transmission electron microscopy (TEM). The nanocomposites exhibited enhanced thermal stability and an increase in glass transition temperature, relative to neat polystyrene. The nanocomposites also exhibited enhanced mechanical properties, which were dependent on the clay loading. Intercalated polystyrene–clay nanocomposites were obtained using the non-polymerizable surfactant-modified clay (cetyltrimethylammonium bromide). Nanocomposites made from mixtures of surfmer-modified and CTAB-modified clays were also prepared, showing intermediate properties. However, when the nanocomposites were prepared in solution only intercalated morphologies were obtained. This was attributed to the competition between the solvent molecules and monomer in penetrating into clay galleries. These nanocomposites also exhibited enhanced thermal stability relative to the virgin polystyrene prepared by the same method. Similar temperatures of degradation (at 50% decomposition) were found for these nanocomposites relative to those prepared by bulk polymerization.

Keywords: Surfmer; Montmorillonite; Nanocomposites

1. Introduction

Inorganic fillers were originally incorporated into polymers to produce cheaper materials. Soon it was discovered that the use of such fillers resulted in improvements in certain polymer properties e.g. stiffness, toughness, chemical resistance, barrier properties, and thermal stability. Such changes in properties depend on several factors: nature and properties of the filler itself of course, but also (and above all) the size and shape of the filler particles, and interactions between the particles and the polymer matrix. For example, with clay fillers, the efficiency of reinforcement is dependent on the aspect ratio (i.e. length to thickness of a clay platelet), the quality of the dispersion, and the adhesion between the matrix and the filler [1,2].

The most abundant natural and inexpensive class of filler materials are the clays. They are extracted as coarse particles made of tactoids (layered structure) which can, in the case of 2:1 phyllosilicates, be exfoliated, giving high aspect ratio particles (sheets). Depending on the degree of exfoliation, the dispersion of clay particles in a polymer matrix can give three types of composite materials, i.e. conventional microcomposites (no exfoliation), intercalated polymer–clay nanocomposites, and exfoliated polymer–clay nanocomposites [1–7].

* Corresponding author. Tel.: +27 21 808 3172; fax: +27 21 808 4967.
E-mail address: rds@sun.ac.za (R.D. Sanderson).

0032-3861/$ - see front matter © 2006 Elsevier Ltd. All rights reserved.
doi:10.1016/j.polymer.2006.07.072

Exfoliated nanocomposites generally have exceptional properties relative to all the other composites. The term nanocomposite describes a two-phase material in which one of the phases is dispersed in the second one on a nanometer scale [6]. Dispersion of clay layers into exfoliated monolayers in non-hydrophilic polymers is hindered by the intrinsic incompatibility of hydrophilic layered silicates with hydrophobic polymers and the inherent tendency to form face-to-face stacks in agglomerated tactoids due to high interlayer cohesive energy. However, as was first demonstrated by the Toyota research group [8,9], the replacement of the inorganic exchangeable cations in the galleries of the native clay by alkylammonium surfactants can compatibilize the clay surface with hydrophobic polymers. The first successful nanocomposite, reported by the Toyota research group [10,11], was in the form of a polyamide 6/clay nanocomposite obtained by *in situ* intercalative polymerization, a method viable for production on industrial scale. The use of organoclays as a route to nanocomposite formation has been extended to other polymer systems, including epoxies, polyurethanes, polyimides, nitrile rubber, polyesters, polypropylene, polystyrene, and polysiloxanes [3]. There is growing interest in the surface chemistry of clays in pursuit of nanocomposites synthesized using specific monomers, prepolymers, and polymer melts [2].

The extent of clay dispersion in polystyrene–clay nanocomposites has mainly been governed by the type of clay, surfactant used in the modification of clay, and the synthesis method. The commonly used clays are montmorillonite (MMT), hectorite, and saponite [1]. Melt intercalation [12–16] and *in situ* intercalative polymerization [17–23] synthesis methods have been used extensively. Surfactants used for the modification of clay for the preparation of polystyrene–clay nanocomposites range from alkyl- and aromatic-containing ammonium surfactants [6,7,12–14,16,23–31] to alkyl phosphonium surfactants [31], and polymerizable surfactants (surfmers) [7,20–23,31–34]. Many researchers have used benzene ring-containing surfactants and vinyl benzyl-containing surfmers, mainly because the benzene ring of the surfactants interacts by van der Waals forces with the benzene rings of styrene and polystyrene [16,21]. In most cases, the use of conventional surfactant resulted in intercalated polystyrene–clay nanocomposites. On the contrary, the use of surfmers generally resulted in exfoliated polystyrene–clay nanocomposites. This has generally been attributed to the copolymerization between styrene and the surfmers inside the clay galleries that causes extensive movement of the clay layers, resulting in exfoliated nanocomposites [22]. In most cases H-type (polymerizable group located in the hydrophilic head) benzene ring-containing surfmers have been used for the modification of clay. The use of non-benzene-ring-containing surfmers has not yet been extensively investigated.

In the work presented in this paper, acrylate-containing surfmers were used to modify clay for the synthesis of polystyrene–clay nanocomposites, using the *in situ* intercalative polymerization technique. It is believed that the polarity of the acrylate group results in greater interactions with the clay surface [14]. A non-polymerizable surfactant with a similar structure was also used to prepare nanocomposites according to the same method so as to understand better the role played by the acrylate group on the final composite structure and properties. Whereas mostly H-type surfmers have been reported in the literature, this study focuses on two acrylic based T-type surfmers (polymerizable group located in the hydrophobic tail) and their use in the preparation of polystyrene-based clay nanocomposites.

2. Experimental section

2.1. Materials

Sodium montmorillonite clay (i.e. MMT clay containing primarily Na^+ ions in the interlayer space) was obtained from Southern Clay Products, Inc. (USA). It is a fine powder with an average particle size of 13 μm^3 by volume in the dry state, with a cation exchange capacity of 92.6 mequiv/100 g of clay. Stabilized styrene monomer was obtained from Aldrich. The stabilizer was removed by washing with a 3 wt% KOH solution followed by distillation under reduced pressure at 30 °C. Azobisisobutyronitrile (AIBN) was purchased from Aldrich and was purified by recrystallization from hot methanol. Cetyltrimethylammonium bromide (CTAB) was obtained from Aldrich (assay 95%) and used without further purification. The synthesis of the surfmers (11-acryloyloxyundecyl)dimethyl(2-hydroxyethyl)ammonium bromide (hydroxyethyl surfmer) and (11-acryloyloxyundecyl)dimethylethylammonium bromide (ethyl surfmer) has been reported elsewhere [35].

2.2. Ion exchange of Na^+-MMT with surfactants

Na^+-MMT (3 g, 2.780 mequiv) was dispersed in 250 ml of deionized water under vigorous stirring (700 rpm). A solution of hydroxyethyl surfmer (1.426 g, 3.615×10^{-3} mol) or ethyl surfmer (1.368 g, 3.615×10^{-3} mol) or CTAB (1.318 g, 3.615×10^{-3} mol) in 100 ml of deionized water was slowly added to the dispersion, under continuous stirring. The resultant dispersion was stirred for a further 6 h. The dispersion was then filtered and the obtained cake was thoroughly washed with deionized water. Samples of the filtrate were taken at regular intervals and tested with a solution of 0.1 M $AgNO_3$ for the presence of released bromide counterions. Washing was discontinued only when the filtrate did not give a positive test to $AgNO_3$. The washed cake was dried overnight under reduced pressure at 40 °C, ground in a mortar and pestle, and sieved through a 63-μm mesh to yield very fine, dry powder (modified MMT clay).

2.3. Reverse ion exchange

Three grams of polymer–clay nanocomposite and 0.9 g of LiCl were dissolved in 240 ml of THF and refluxed at 70 °C for 48 h. The reaction was stopped and the polymer precipitated in methanol and dried. GPC analysis was performed on polymer solutions in THF (8 mg/ml).

2.4. Synthesis of polystyrene–clay nanocomposites

2.4.1. Polymerization in bulk

Nanocomposites were prepared using clay modified with hydroxyethyl surfmer, ethyl surfmer, or CTAB. All the polystyrene–MMT nanocomposites prepared by bulk polymerization were prepared according to the following procedure. Modified MMT clay (0.250 g) and AIBN (0.024 g, 1.46×10^{-4} mol) were added into a Schlenk tube containing freshly distilled styrene monomer (4.750 g, 0.046 mol). The mixture was degassed by three freeze–vacuum–thaw cycles, then stirred, and sonicated in a cold water bath for 4 h. The Schlenk tube was placed in an oil bath at 60 °C for 72 h. The obtained polymer was dissolved in chloroform, precipitated into methanol, filtered, and dried, yielding an off-white powder.

2.4.2. Polymerization in solution

The method used to synthesize the polystyrene–clay nanocomposites in solution was similar to the bulk polymerization except that a 15 wt% solution of monomer in toluene was used, and polymerization was carried out at 80 °C for 24 h.

2.5. Measurements

Proton nuclear magnetic resonance spectroscopy (^{1}H NMR) was performed at 20 °C using a Varian VXR-300 MHz and a Varian Inova-600 MHz NMR spectrometers. Fourier-transform infrared (FT-IR) spectroscopy was carried out on a Nexus FT-IR instrument, by averaging 32 scans with a wave number resolution of 4 cm^{-1}. Thermogravimetric analysis (TGA) measurements were done on a Perkin Elmer TGA 7 instrument. Samples of less than 20 mg were used for all analyses and were analyzed from ambient temperature to 600 °C at 20 °C/min heating rate. All TGA analyses were done under air atmosphere. Gel permeation chromatography (GPC) was carried out using a Waters 600E system controller equipped with a Waters 610 Fluid Unit pump and a Waters 410 Differential Refractometer as detector. THF was used as an eluent. Samples were filtered through a 0.45-μm filter membrane prior to analysis.

Mechanical properties of the nanocomposites were determined by dynamic mechanical analysis (DMA) using a Perkin Elmer DMA 7e instrument that employs a parallel plate measuring system equipped with a 1-mm probe. Sample discs were prepared by pressing using a hydraulic press. Samples were cooled to −20 °C for 1 min, then the temperature was raised to 200 °C at a heating rate of 5 °C/min, under nitrogen atmosphere, and using a frequency of 1 Hz.

Small angle X-ray scattering (SAXS) measurements were performed at 298 K in a transmission configuration. A copper rotating anode X-ray source (functioning at 4 kW) with a multilayer focusing "Osmic" monochromator giving high flux (10^8 photons/s) and punctual collimation was used. An "image plate" 2D detector was used. Diffraction curves were obtained giving diffracted intensity as a function of the wave vector q. The calculation of q values is described elsewhere [36].

Transmission electron microscopy (TEM) was used to directly visualize the clay particles' morphology in the nanocomposite. Bright field TEM images were recorded on a JEM 200CX (JEOL Tokyo, Japan) transmission electron microscope at an accelerating voltage of 120 kV. Prior to analysis, samples of polystyrene–clay nanocomposites were stained with OsO_4, then embedded in epoxy resin and cured for 24 h at 60 °C. The embedded samples were then cut into slices of a nominal thickness of 100 nm using an ultra-microtome with a diamond knife on a Reichert Ultracut S ultra-microtome at room temperature. The sections were transferred from water at room temperature onto a 300-mesh copper grid.

3. Results and discussion

3.1. Modification of clay using hydroxyethyl and ethyl surfmers

The structure of Na^+-MMT comprises layers made up of one octahedral alumina sheet sandwiched between two tetrahedral silica sheets. About one in six of the aluminum ions in the octahedral layers of Na^+-MMT is isomorphously substituted in the sheet structure by magnesium or other divalent ions; this results in negative charges that are in turn counter-balanced by Na^+ cations residing in the interlayer space [2]. The Na^+ ions in the gallery space can be ion exchanged by an organic cation (surfactant) to yield surfactant-modified clay.

The two polymerizable surfactants (i.e. ethyl and hydroxyethyl surfmers) were used to ion exchange sodium cations in Na^+-MMT. In all cases the amount of surfmer used was in excess (1.3:1) with regards to the cation exchange capacity (CEC). TGA was then used to determine the amount of ion-exchanged surfactant [21,33,37–39] (see Fig. 1). For all samples analyzed, the total amount of adsorbed surfmer was close to 70% of the CEC value (i.e. 92.6 mequiv/100 g clay) and the total quantity of adsorbed surfmer was found to be independent of temperature and shear rate.

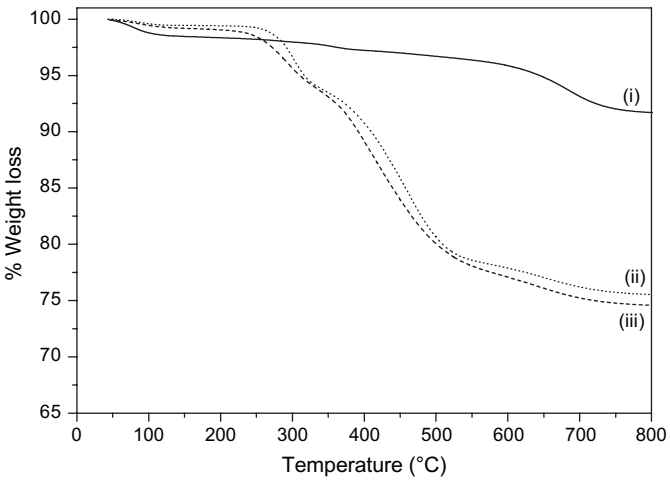

Fig. 1. TGA thermograms of Na^+-MMT (i) before, and after ion exchange with (ii) ethyl surfmer, and (iii) hydroxyethyl surfmer.

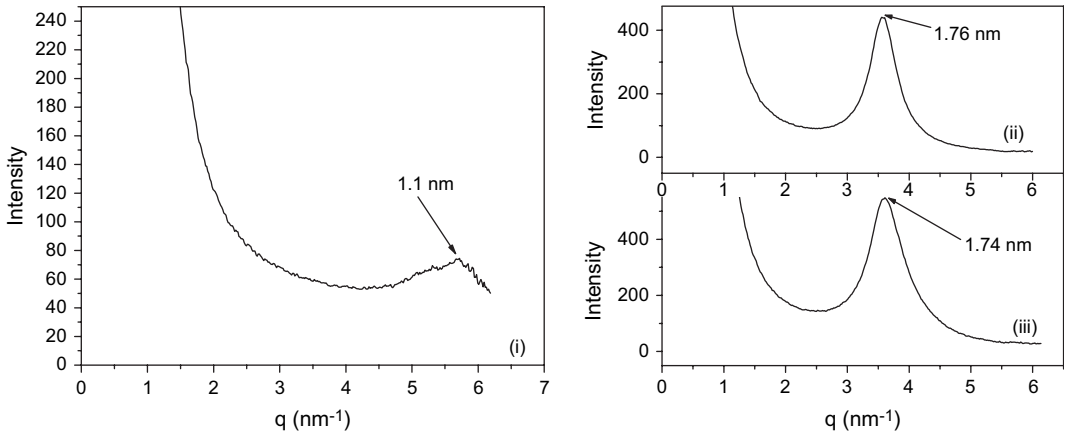

Fig. 2. SAXS patterns of (i) Na^+-MMT, (ii) hydroxyethyl-MMT, and (iii) ethyl-MMT.

The changes in the interlayer distance (d spacing) before and after the ion exchange process were monitored using SAXS measurements. The d spacings were calculated using the formula: $d = 2\pi/q$ (where q is the wave vector; associated Bragg's peak position). The d spacing found for Na^+-MMT clay, 1.1 nm, was comparable to the values reported in literature [6,21–23,40]. As shown in Fig. 2, an increased interlayer distance was found with modified clays relative to unmodified clay. The interlayer distances of the two surfmer-modified clays were similar (i.e. 1.76 and 1.74 nm for hydroxyethyl-MMT and ethyl-MMT, respectively). The results obtained show that the interlayer distance of modified clays is mainly governed by the length of the alkyl chain of the modifying surfactants [22] and the clay charge density [2]. Thus SAXS patterns also confirmed the TGA results described above, showing that the ion exchange reaction had indeed taken place.

The FT-IR spectra of the modified clays showed the appearance of new bands relative to unmodified clay and surfmers (see Fig. 3 and Table 1).

In the spectra of both the modified and unmodified clays, the intense peak at 1045 cm^{-1} and the two bands at 468 and 524 cm^{-1} were assigned to Si–O bonds' stretching and Si–O bonds' bending, respectively [6,33]. The bands around 1632 and 3600 cm^{-1} are due to the hydroxyl groups in the clay

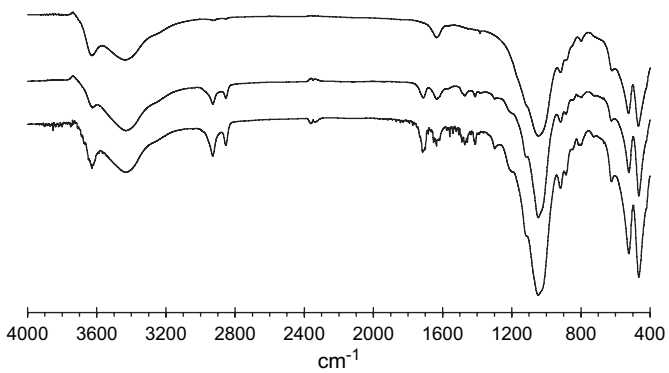

Fig. 3. FT-IR spectra of Na^+-MMT (top), ethyl-MMT (middle), and hydroxyethyl-MMT (bottom).

[6,33,41]. The other additional bands observed in the spectrum of the modified clays arise from surfactant bonds' stretching or bending. The absorption peak of the carbonyl group in the surfmer-modified clays shifts to a lower wave number, i.e. 1714 cm^{-1}, relative to 1721 and 1725 cm^{-1} in the hydroxyethyl and ethyl surfmers, respectively. This could be due to interactions between the surfmer's acryloyl group and the clay surface [41], most likely via hydrogen bonding with the hydroxyl groups localized on the edges of the clay surface.

3.2. Preparation of polystyrene–clay nanocomposites by free-radical polymerization

Polystyrene–clay nanocomposites were prepared by free-radical polymerization in bulk, in the presence of surfmer-modified clays. Nanocomposites were also prepared using CTAB-modified clay (CTAB-MMT). CTAB was used as a classical surfactant with a structure comparable to both of the studied surfmers, so as to show the effect of the polymerizable group on the nanocomposites' morphologies and properties. A polystyrene devoid of any clay filler was also prepared under the same polymerization condition, as a standard.

FT-IR spectra of the synthesized polystyrene–clay nanocomposites showed the presence of all the functional groups expected, i.e. absorptions due to clay, surfactants, and polystyrene.

As shown in Fig. 4a, no peak was observed by SAXS for the polystyrene–(ethyl-MMT) nanocomposites, indicating total exfoliation for clay content up to 18.5 wt%, as confirmed

Table 1
FT-IR results of Na^+-MMT, hydroxyethyl-MMT, and ethyl-MMT

Assigned groups	Wavelength (cm^{-1})		
	Na^+-MMT	Hydroxyethyl-MMT	Ethyl-MMT
Al–O	625	627	627
Si–O	524, 468, 1045	524, 466, 1049	524, 466, 1049
$-CH_3$		1411	1408
$-CH_2-$		1471	1468
$>C=O$		1714	1714
–C–H		2845, 2929	2853, 2928
O–H	1632, 3438, 3625	1632, 3430, 3633	1636, 3430, 3633

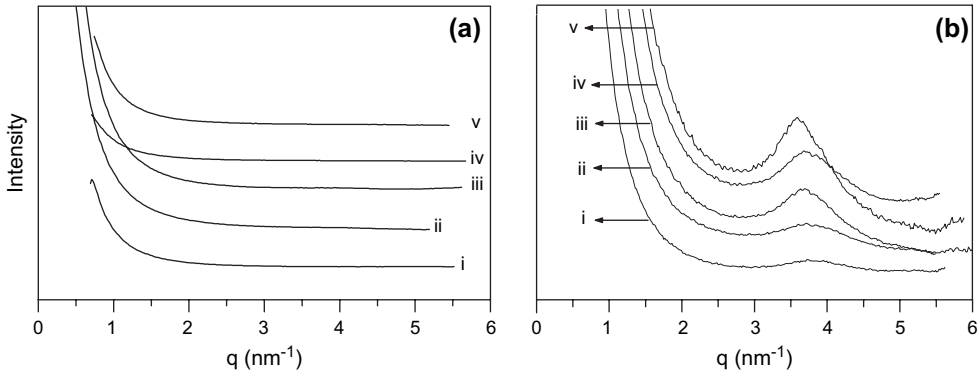

Fig. 4. SAXS patterns of (a) polystyrene–(ethyl-MMT) nanocomposites with 2.1 (i), 3.7 (ii), 5.7 (iii), 7.7 (iv), and 18.5 wt% (v) of clay; and (b) polystyrene–(hydroxyethyl-MMT) nanocomposites with 1.5 (i), 5.3 (ii), 7.1 (iii), 18.5 (iv), and 21.3 wt% (v) of clay.

by TEM (cf. Fig. 6a). This was unexpected as previous research where exfoliation was obtained, had only been carried out at low clay contents (i.e. less than 10 wt%) [21]. As shown in Fig. 4b, the SAXS patterns of polystyrene–(hydroxyethyl-MMT) nanocomposites showed a broad peak around 3.6–3.8 nm^{-1}, which became broader as the clay content decreased. Peak broadening can be attributed to either a partial exfoliation [42], disordering in the clay tactoids or an insufficient sensitivity of the apparatus as the clay level decreases. As shown by TEM (cf. Fig. 6b), the partially exfoliated structure (intercalated/exfoliated) was confirmed for the polystyrene–(hydroxyethyl-MMT) nanocomposite. An intercalated structure was found by TEM and SAXS (cf. Fig. 5) for the polystyrene–(CTAB-MMT) nanocomposites, in agreement with similar results reported in the literature [21].

The difference in the structure of the nanocomposites obtained using the two surfmer-modified clays is most likely a result of thermodynamic effects. Here it is necessary to look at the interactions between clay and polymer, clay and surfactant, and between polymer and surfactant. An optimum balance of all these interactions generally leads to an exfoliated nanocomposite [38]. The ethyl surfmer can interact with clay through electrostatic interactions and hydrogen bonding. It interacts with styrene–polystyrene through dispersion forces because of the tail hydrophobicity. The hydroxyethyl surfmer has the same characteristics, except that it possesses an additional polar 2-hydroxyethyl group, which implies more interaction with clay [23], leading to an imbalance, hence allowing only a partial exfoliation.

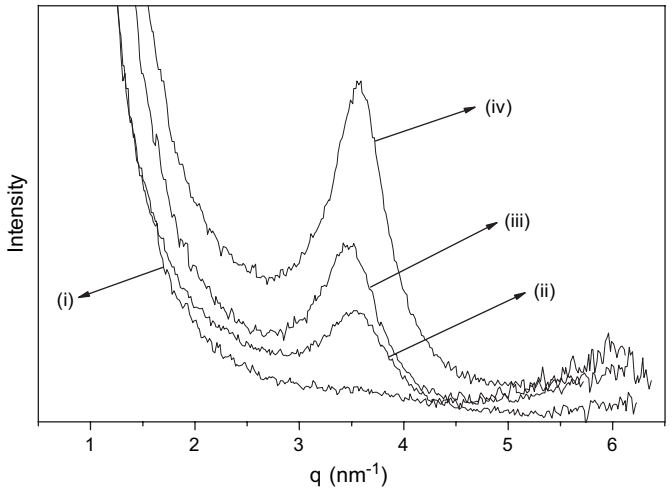

Fig. 5. SAXS patterns of (a) polystyrene–(CTAB-MMT) nanocomposites with 0.8 (i), 1.2 (ii), 3.5 (iii), and 6.0 wt% (iv) of clay.

3.3. TGA analysis of polystyrene–clay nanocomposites

The thermal stabilities of all the polystyrene–clay nanocomposites prepared were higher than that of virgin polystyrene, which is in agreement with literature [21–23,26,29]. The enhancement in thermal stability increased only slightly as the clay loading increased. The improvement in thermal stability of polymer–clay nanocomposites is explained by the formation of clay char which acts as mass transport barrier and insulator between the polymer and the superficial zone where the polymer decomposition takes place [22,30]. The thermal stability has also been attributed to restricted thermal motions of the polymer localized in the galleries [43].

Fig. 7 shows that the thermal stabilities of the nanocomposites are quite similar regardless of the extent of clay dispersion. Surprisingly, the polystyrene–(CTAB-MMT) nanocomposite (intercalated) was found to be the most thermally stable, followed by the polystyrene–(hydroxyethyl-MMT) nanocomposite (intercalated/exfoliated) and lastly the polystyrene–(ethyl-MMT) nanocomposite (exfoliated). Giannelis found similar unexpected results with polyimide–clay nanocomposites (10 wt% clay loading), for which intercalated structure displayed higher thermal stabilities than the exfoliated one [44]. However, our results disagree with Zhang's findings that the exfoliated polystyrene–clay nanocomposites had better thermal properties relative to the intercalated ones [22]. We believe that there is a need to have several closely packed layers of clay (stacked layers) in order to provide an efficient barrier between the thermal degradation zone and the underlying flammable material that is being gasified. This idea suggests that the intercalated structures will be more stable than the exfoliated and the partially exfoliated polystyrene–clay nanocomposites, as is observed in this case. This correlates with the findings of Gilman et al. [45], who observed that an

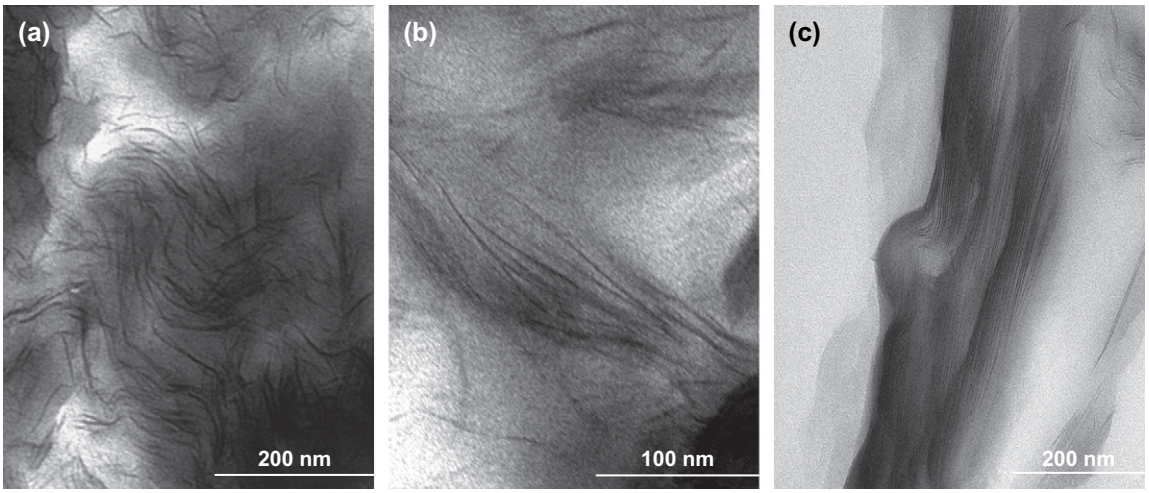

Fig. 6. TEM images of (a) exfoliated polystyrene–(ethyl-MMT) nanocomposite, (b) partially exfoliated polystyrene–(hydroxyethyl-MMT) nanocomposite, and (c) intercalated polystyrene–(CTAB-MMT) nanocomposite at 5.7, 5.3 and 6.0 wt% clay content, respectively.

exfoliated structure does not necessarily bring about the best improvement in terms of flammability. The degradation temperature of the surfactants alone may also have an influence on the degradation temperature of the nanocomposites as it was observed. Gilman stated that the degradation of the surfactant itself can accelerate the flammability due to the release of degradation products. Thus, intercalated morphologies would effectively minimize this effect by reducing the dispersion of the surfactant degradation products. Chigwada et al. also found that addition of a highly volatile phosphate to a polystyrene–clay nanocomposites resulted in its thermal stability [29]. Here the onset of degradation of the surfactants taken at 10% weight loss, [29], was found to be 240 °C for ethyl surfmer, 270 °C for hydroxyethyl surfmer and 261 °C for CTAB. Thus the intercalated and partially intercalated structures for CTAB and hydroxyethyl surfmer-based nanocomposites together with the high degradation temperatures of the surfactants could have resulted in a better thermal stability relative to the ethyl surfmer-based exfoliated nanocomposites.

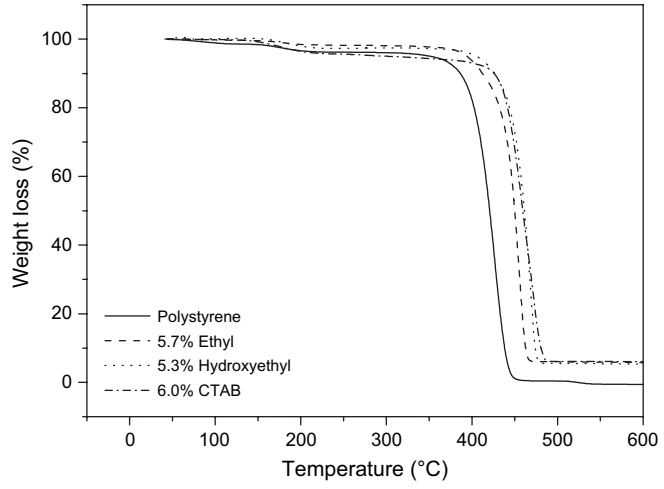

Fig. 7. TGA plots of three different nanocomposites with similar clay loadings. The legend indicates clay percentage and the type of surfactant used to modify the clay.

3.4. DMA analysis of polystyrene–clay nanocomposites

DMA analysis was used to evaluate the effect of clay loading and degree of exfoliation on the thermomechanical properties of the polystyrene–clay nanocomposites. Exfoliated nanocomposites showed better mechanical properties relative to the other nanocomposites. An increase in the storage modulus was observed as clay loading increased. A similar trend has been previously reported in literature [21,24,33,39,46]. As shown in Fig. 8a, the exfoliated polystyrene–(ethyl-MMT) nanocomposite has a higher storage modulus relative to the partially exfoliated polystyrene–(hydroxyethyl-MMT) nanocomposite at the same clay loading. The small peak that formed just before the drop in the storage modulus of polystyrene–(ethyl-MMT) nanocomposite is due to stress relaxation [47]. The enhancement in storage modulus is caused by the high aspect ratio of the dispersed clay and the interaction between the polymer chains and clay layers, resulting in a decrease in the polymer segments' mobility near the polymer–clay interface [48].

Fig. 8b shows peak broadening and a shift of the tan δ peaks of the nanocomposites to higher temperatures, relative to polystyrene. These shifts have been reported before, and are attributed to a restricted chain mobility brought about by the clay nanofiller [49,50]. The glass transition temperatures of the nanocomposites were found to be higher than those of neat PS, and increased slightly with the clay content. This is in accordance with the assumption that clay is linked to the PS matrix via copolymerization of the acrylic groups belonging to the surfmers, themselves attached to the clay surface via ionic bonds. Since many surfmer molecules are bound to each clay platelet, surfmer-modified clay platelets can be assimilated as multi-crosslinking bridges between many PS chains, thus restricting the overall polymer motion [51]. The resulting increase in the T_g is in accordance with results reported by

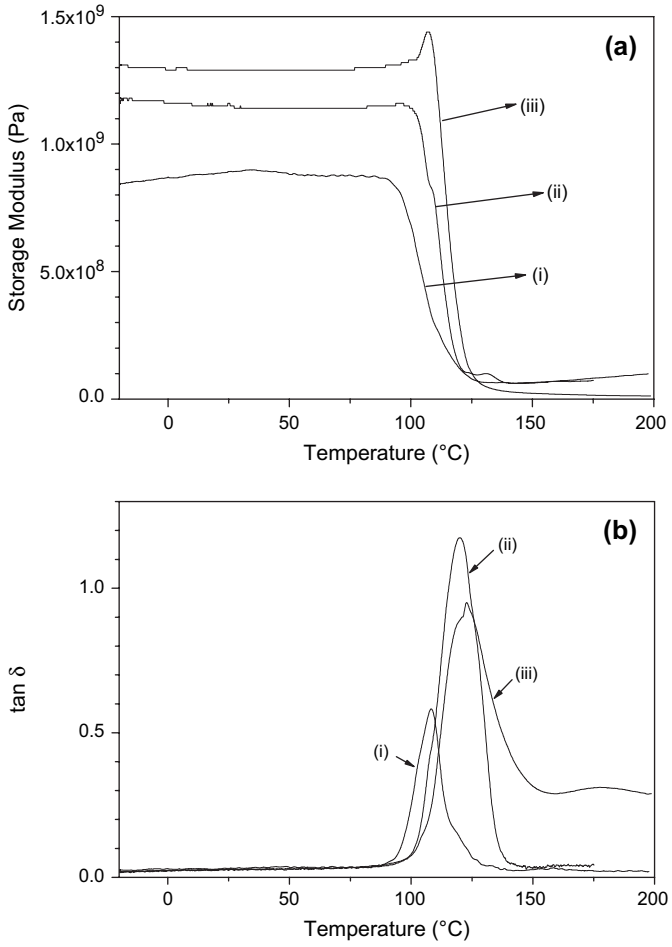

Fig. 8. Variation of (a) storage modulus and (b) tan δ with temperature for (i) polystyrene, (ii) polystyrene−(hydroxyethyl-MMT) nanocomposite, and (iii) polystyrene−(ethyl-MMT) nanocomposite. Both nanocomposites contain 18.5 wt% clay loading.

Tyan et al. [46], whereas it diverges from Fu and Qutubuddin [21], who reported a decrease in T_g with an increase in clay loading. The latter attributed the decrease in T_g to the high viscosity of the organophilic MMT−styrene dispersion that affects the diffusion of initiator molecules and chain propagation during polymerization, thus favoring termination. This latter phenomenon apparently did not occur in the present work, as the molecular masses of all nanocomposites were found to be higher than that of the virgin polystyrene (cf. Table 2).

The high molecular masses were attributed to a low probability of termination caused by low polymerization temperature (i.e. 60 °C) and high viscosity associated with bulk polymerization. The high viscosity is further exacerbated by the modified clay dispersion. Further, termination is not possible between two propagating chains situated on opposite sides of a clay platelet, hence the high molecular masses of nanocomposites relative to virgin polystyrene. Reverse ion exchange reactions were carried out on both surfmer-based nanocomposites so as to ascertain whether copolymerization of styrene with the reactive surfactants has an impact on the molecular weight. This was done in order to show whether there is a difference or not in the molecular weights of

Table 2
GPC results of PS and PS nanocomposites obtained by polymerization in bulk

Sample	Clay content (wt%)	M_n (g/mol) ($\times 10^3$)	M_w (g/mol) ($\times 10^3$)	M_w/M_n
Polystyrene	–	170	510	3.1
Polystyrene−(hydroxyethyl-MMT) nanocomposite	1.5	230	740	3.2
	5.3	240	690	2.8
	7.1	200	860	4.2
	18.5	170	440	2.6
	21.3	400	1190	3.0
Polystyrene−(ethyl-MMT) nanocomposite	2.1	190	690	3.7
	3.7	190	580	3.1
	5.7	210	630	2.9
	7.7	140	840	5.9
	18.5	240	1120	4.7
Polystyrene−(CTAB-MMT) nanocomposite	0.8	120	480	4.0
	1.2	80	540	6.8
	3.5	80	540	6.8
	6.0	80	540	6.4

polymers formed inside and outside the clay galleries. GPC chromatograms of a polystyrene−(ethyl-MMT) nanocomposite (containing, respectively, 5.7 and 5.3 wt% of clay) before and after reverse ion exchange reaction are shown in Fig. 9. Very little differences in the molecular masses were observed before and after reverse ion exchange. Assuming that any clay aggregates were eliminated during the filtration process prior to analysis, the similarity in the molecular weight distributions can be interpreted in two ways, namely (1) grafted and non-grafted polymer chains have the same weight distribution or (2) no true copolymerization of styrene with surfmers occurred in the course of polymerization. The first hypothesis is more relevant, taking into account the changes in the nanocomposites' morphology/properties observed when the surfactant contained an acrylic polymerizable group. Extensive movement of clay platelets during copolymerization of the ion-exchanged surfmers with the growing polystyrene main chain has been reported as the driving force of exfoliation [22].

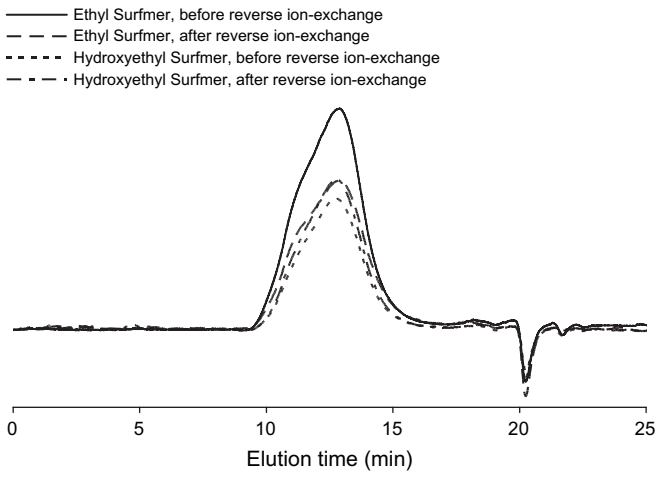

Fig. 9. GPC traces (RI detection) of polystyrene−(ethyl-MMT) nanocomposite and polystyrene−(hydroxyethyl-MMT) nanocomposite before and after reverse ion exchange reaction.

3.5. Preparation of polystyrene–clay nanocomposites using mixtures of modified clays

Exfoliated nanocomposites are mainly achieved by the use of surfmer-modified clays. However, surfmers are generally expensive to make, increasing drastically the production cost of exfoliated nanocomposites [16]. To our knowledge, there is no literature available on the use of mixtures of classical surfactant-modified clay and surfmer-modified clay to synthesize exfoliated polymer–clay nanocomposites. In the present work, mixtures of (i) ethyl-MMT clay and CTAB-MMT clay and (ii) hydroxyethyl-MMT clay and CTAB-MMT-modified clays were used, in different proportions, in bulk polymerization of styrene. The molecular masses were found to be of the same range as those obtained when clay that was modified with only one surfactant was used (see Table 3).

SAXS analysis was carried out on the resulting polymers, the objective being to determine whether exfoliation took place even while using only a fraction of surfmer-modified clay. The clays were thoroughly mixed in known ratios (percentage by mass of surfmer-modified clay to classical surfactant-modified clay), and the total mass of the modified clay mixtures relative to the amount monomer was kept constant at 5% in all cases. As shown by SAXS patterns of polystyrene–(hydroxyethyl-MMT–CTAB-MMT) nanocomposites (cf. Fig. 10a), predominantly partially exfoliated structures were obtained, for all modified clay ratios investigated. In the case of polystyrene–(ethyl-MMT–CTAB-MMT) nanocomposites, a similar partially exfoliated structure was obtained for a 25/75 modified clay ratio (see Fig. 10b (ii)). With ratios 50/50 and 75/25, no noticeable peak was observed in the SAXS patterns. This may be due to a totally exfoliated morphology, the exfoliation of ethyl-MMT promoting the exfoliation of CTAB-MMT neighbours. This is difficult to explain, considering the accepted driving force for clay exfoliation, unless a small but significant amount of surfmer may have partitioned between the two clays by moving through the monomer–polymer medium.

Table 3
GPC results of polystyrene and polystyrene nanocomposites obtained using mixtures of modified clay

Sample	Ratio of modified clays	M_n (g/mol) ($\times 10^3$)	M_w (g/mol) ($\times 10^3$)	M_w/M_n
Polystyrene	–	170	510	3.1
Polystyrene–(hydroxyethyl-MMT–CTAB-MMT) nanocomposites	100/0	230	690	2.8
	75/25	60	290	5.3
	50/50	40	230	5.6
	25/75	60	300	5.1
	0/100	80	540	6.8
Polystyrene–(ethyl-MMT–CTAB-MMT) nanocomposites	100/0	210	630	2.9
	75/25	40	230	5.8
	50/50	80	400	5.2
	25/75	60	450	7.9
	0/100	80	540	6.8

The thermal stability of polystyrene–(hydroxyethyl-MMT–CTAB-MMT) nanocomposites is comparable to that of the partially exfoliated hydroxyethyl-MMT polystyrene nanocomposites. This was expected, as both structures were of the same morphology, i.e. exfoliated/intercalated. On the other hand, the polystyrene–(ethyl-MMT–CTAB-MMT) nanocomposite was found to be thermally more stable than the ethyl-MMT polystyrene. This improvement is remarkable as shown by SAXS results, clay was predominantly exfoliated in the ethyl-MMT–CTAB-MMT polystyrene nanocomposite (cf. Fig. 11). This result points out a new and convenient way of preparing nanocomposites with optimal thermal stability and mechanical properties using *in situ* intercalative polymerization of surfactant-modified and surfmer-modified clay mixtures.

3.6. Preparation of polystyrene–clay nanocomposites by polymerization in solution

Preparation of nanocomposites by polymerization in solution (toluene) was carried out in order to show the solvent's

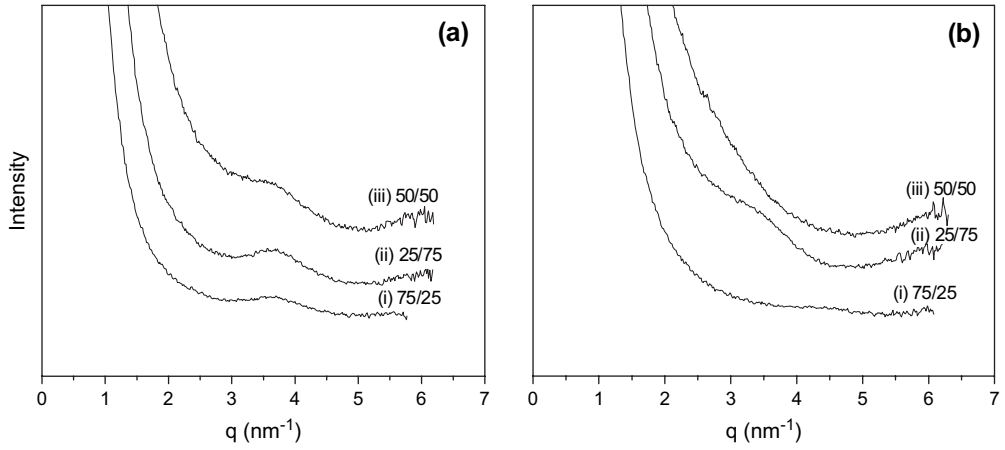

Fig. 10. SAXS patterns of polystyrene–clay nanocomposites obtained using mixtures of modified clays: (a) polystyrene–(hydroxyethyl-MMT–CTAB-MMT) nanocomposites (ratios hydroxyethyl-MMT/CTAB-MMT clay); (b) polystyrene–(ethyl-MMT–CTAB-MMT) nanocomposites (ratios ethyl-MMT/CTAB-MMT clay).

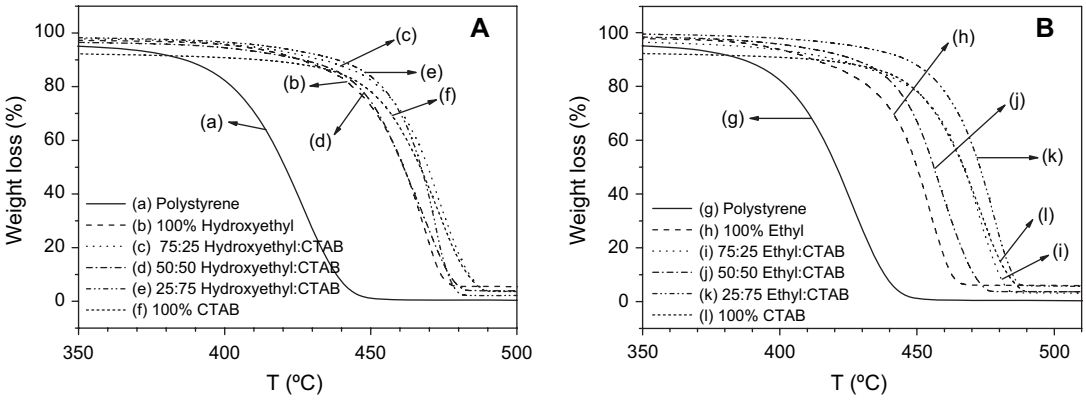

Fig. 11. TGA plots of polystyrene–clay nanocomposites at the same clay loading prepared using mixtures of modified clays. The legend indicate the ratio of surfmer to CTAB in the modified clay mixture, the thermogram of neat polystyrene was inserted as a reference.

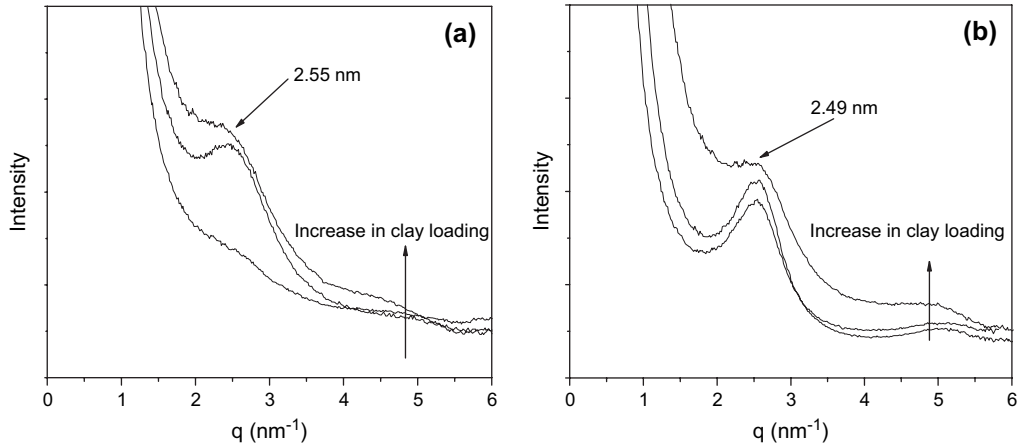

Fig. 12. SAXS patterns of (a) polystyrene–(hydroxyethyl-MMT) nanocomposites containing 2, 11, and 17 wt% clay and (b) polystyrene–(ethyl-MMT) nanocomposites containing 1.5, 9.7, and 14 wt% clay. The arrows in the diagrams show the directions of clay increase.

effect on the final polystyrene–clay nanocomposite's structure and its thermal properties.

SAXS patterns for both polystyrene–(hydroxyethyl-MMT) nanocomposites and polystyrene–(ethyl-MMT) nanocomposites showed them to be intercalated nanocomposites (cf. Fig. 12). Exfoliation was not achieved and this has been attributed to the competition between the monomer and the solvent (toluene) for intercalation into the clay galleries [12], thus decreasing the interfacial polymer density inside the clay galleries. The resulting pressure exerted by the polymer chains on the clay platelets is insufficient to promote clay exfoliation [52], resulting in intercalated structure.

As shown by SAXS (cf. Fig. 12), the average interlayer distances for the polystyrene–(hydroxyethyl-MMT) and polystyrene–(ethyl-MMT) were 2.55 and 2.49 nm, respectively. These interlayer distances are greater than those reported by Akelah and Moet (i.e. between 1.72 and 2.45 nm) [19] for polystyrene–clay nanocomposites prepared by *in situ* solution polymerization using a different polymerizable surfactant-modified clay.

When compared to bulk polymerization, solution polymerization yielded polymers with lower molecular weights and narrower polydispersity indexes (cf. Table 4). This is due to lower viscosity, higher diffusion rates, and a higher concentration of propagating radicals (due to a higher temperature of polymerization) in solution polymerization, hence favoring termination of growing chain.

Nanocomposites prepared by polymerization in solution were thermally more stable than neat polystyrene prepared with the same procedure, and the thermal stability improved

Table 4
GPC results of polystyrene and polystyrene nanocomposites obtained from solution polymerization

Sample	Clay content (wt%)	M_n (g/mol) ($\times 10^3$)	M_w (g/mol) ($\times 10^3$)	M_w/M_n
Polystyrene	0	10.2	19.0	1.9
Polystyrene–(hydroxyethyl-MMT) nanocomposite	2	7.9	14.6	1.9
	11	6.4	14.6	2.3
	17	7.1	15.9	2.2
Polystyrene–(ethyl-MMT) nanocomposite	1.5	8.1	15.2	1.9
	9.7	8.3	15.4	1.9
	14	7.8	14.6	1.9

slightly as the clay loading increased. The temperatures of onset decomposition taken at 10% weight loss [29] of the nanocomposites prepared in solution were found to be lower than those of the nanocomposites prepared in bulk, showing that the temperature of the onset of thermal decomposition was in these cases related to the difference in the molar masses of the polystyrene matrix [53]. Nevertheless, nanocomposites prepared with both methods (i.e. polymerization in solution and polymerization in bulk) had lost 50% of their original weight at the same temperature.

4. Conclusions

Hydroxyethyl and ethyl surfmers were used for the modification of clay and, subsequently, for the preparation of polystyrene–clay nanocomposites by free-radical polymerization in bulk and in solution. In bulk polymerization, the use of ethyl-MMT clay resulted in fully exfoliated polystyrene–clay nanocomposites, whereas the use of hydroxyethyl-MMT clay gave partially exfoliated (exfoliated/intercalated) nanocomposites. The prepared nanocomposites exhibited improved thermal stability relative to neat polystyrene. The highest thermal stability was found with the intercalated nanocomposite made using CTAB-MMT-modified clay. The nanocomposites also exhibited enhanced mechanical properties which were dependent on the extent of clay dispersion. Nanocomposites prepared using mixtures of modified clays, ethyl-MMT and CTAB-MMT, were found to have mainly exfoliated structures, combined with enhanced thermal stability. When prepared by free-radical polymerization in solution, nanocomposites exhibited better thermal stabilities relative to neat polystyrene. Their molar weights were found to be relatively low, and exclusively intercalated structures were observed. Exfoliation was not achieved in nanocomposites prepared in solution by polymerization and this was attributed to the competition between the solvent molecules and monomer in penetrating into clay galleries.

Acknowledgment

The authors thank the National Research Foundation (NRF) for funding.

References

[1] Alexandre M, Dubois P. Mater Sci Eng 2000;28:1–63.
[2] Rosorff M. Nano surface chemistry. New York, Basel: Marcel Dekker Inc; 2002.
[3] Biswas M, Ray SS. Adv Polym Sci 2001;155:170–221.
[4] Okamoto M. Encyclopedia of nanoscience and nanotechnology. California: American Scientific Publishers; 2004.
[5] Ray SS, Okamoto M. Prog Polym Sci 2003;28:1539–641.
[6] Sadhu S, Bhowmick AK. J Appl Polym Sci 2004;92:698–709.
[7] Pinnavaia P. Appl Clay Sci 1999;15:11–29.
[8] Jordan JW. J Phys Colloid Chem 1949;53:294–306.
[9] Fukushima Y, Inagaki S. J Inclusion Phenom 1987;5:473–82.
[10] Usuki A, Kojima Y, Kawasumi M, Okada A, Fukushima Y, Kurauchi T, et al. J Mater Res 1993;8:1179–84.
[11] Okada A, Fukushima Y, Kawasumi M, Inagaki S, Usuki A, Sugiyama S, et al. USP4,739,007; 1988.
[12] Vaia RA, Giannelis EP. Macromolecules 1997;30:7990–9.
[13] Vaia RA, Jandt KD, Kramer EJ, Giannelis EP. Macromolecules 1995;28:8080–5.
[14] Vaia RA, Giannelis EP. Macromolecules 1997;30:8000–9.
[15] Vaia RA, Ishii H, Giannelis EP. Chem Mater 1993;5:1694–5.
[16] Robello DR, Yamaguchi N, Blanton T, Barnes C. J Am Chem Soc 2004;126:8118–9.
[17] Okamoto M, Morita S, Kim HY, Kotaka T, Tateyama H. Polymer 2001;42:1201–6.
[18] Zerda SA, Caskey CT, Lesser JA. Macromolecules 2003;36:1603–8.
[19] Akelah A, Moet A. J Mater Sci 1996;31:3589–96.
[20] Zeng C, Lee LJ. Macromolecules 2001;34:4098–103.
[21] Fu X, Qutubuddin S. Polymer 2001;42:807–13.
[22] Zhang WA, Chen DZ, Xu HY, Shen XF, Fang YE. Eur Polym J 2003;39:2323–8.
[23] Tseng C, Wu J, Lee H, Chang F. J Appl Polym Sci 2002;85:1370–7.
[24] Zhang W, Chen D, Zhao Q, Fang Y. Polymer 2003;44:7953–61.
[25] Park CI, Park OO, Lim JG, Kim HJ. Polymer 2001;42:7465–75.
[26] Yei D, Kuo S, Su Y, Chang F. Polymer 2004;45:2633–40.
[27] Zax DB, Santos DK, Hegemann H, Giannelis EP, Manias E. J Chem Phys 2000;112:2945–51.
[28] Ryu JG, Park SW, Kim H, Lee JW. Mater Sci Eng 2004;24:285–8.
[29] Chigwada G, Wilkie CA. Polym Degrad Stab 2003;80:551–7.
[30] Wang J, Du J, Zhu J, Wilkie CA. Polym Degrad Stab 2002;77:249–52.
[31] Zhu J, Morgan AB, Lamelas FJ, Wilkie CA. Chem Mater 2001;13:3774–80.
[32] Wilkie CA, Zhang J. Polym Degrad Stab 2004;83:301–7.
[33] Xu M, Choi YS, Kim YK, Wang KH, Chung IJ. Polymer 2003;44:6387–95.
[34] Park CI, Kim H, Park OO. Polymer 2004;45:1267–73.
[35] Samakande A, Hartmann PC, Sanderson RD. J Colloid Interface Sci 2006;296:316–23.
[36] Hartmann PC, Dieudonne P, Sanderson RD. J Colloid Interface Sci 2005;284:289–97.
[37] Biasci L, Aglietto M, Ruggeri G, Ciardelli F. Polymer 1994;35:3296–304.
[38] Fornes TD, Hunter DL, Paul DR. Macromolecules 2004;37:1793–8.
[39] Kawasumi M, Hasegawa N, Kato M, Usuki A, Okada A. Macromolecules 1997;30:6333–8.
[40] Wang M, Zhao F, Guo Z, Dong S. Electrochim Acta 2004;1–8.
[41] Choi YS, Ham HT, Chung I. J Chem Mater 2004;16:2522–9.
[42] Morgan AB, Gilman JW. J Appl Polym Sci 2003;87:1329–38.
[43] Bluimstein A. J Polym Sci A 1965;3:2665–73.
[44] Giannelis E. Adv Mater 1996;8:29–31.
[45] Gilman JW, Kashiwagi T, Morgan AB, Harris RH, Brassell LD, VanLandingham MR, et al. NISTIR 6531; 2000. p. 1–55.
[46] Tyan H, Wei K, Hsieh T. J Polym Sci Part B Polym Phys 2000;38:2873–8.
[47] Menard KV. Dynamic mechanical analysis. CRC Press; 1999.
[48] Luo J, Daniel IM. Compos Sci Technol 2003;63:1607–16.
[49] Noh MW, Lee DC. Polym Bull 1999;42:619–26.
[50] Yu Y, Yeh J, Liou S, Chang Y. Acta Mater 2004;52:475–86.
[51] Akade A, Usuki A. Mater Sci Eng 1995;C3:109–15.
[52] Gardebien F, Brédas J, Lazzaroni R. J Phys Chem B 2005;109:12287–96.
[53] Bicerano J. Prediction of polymer properties. 2nd ed. New York: Dekker; 1996.